Engineered Antifouling Microtopographies: An Energetic Model That Predicts Cell Attachment

Joseph T. Decker,[†] Chelsea M. Kirschner,[‡] Christopher J. Long,[§] John A. Finlay,[‖] Maureen E. Callow,[‖] James A. Callow,[‖] and Anthony B. Brennan*[,†]

[†]Department of Materials Science and Engineering, University of Florida, Gainesville, Florida 32611-6400, United States
[‡]Department of Chemical and Biological Engineering, University of Colorado Boulder, Boulder, Colorado 80309, United States
[§]NanoScience Technology Center, University of Central Florida, Orlando, Florida 32816, United States
[‖]School of Biosciences, University of Birmingham, Birmingham, U.K.
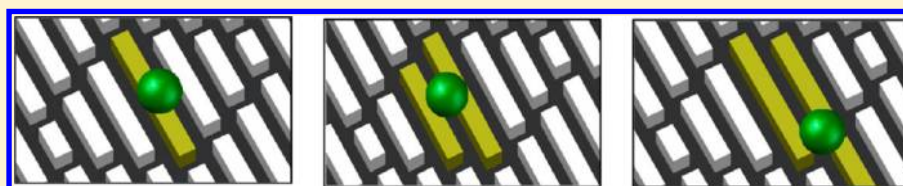
ABSTRACT: We have developed a model for the prediction of cell attachment to engineered microtopographies based on two previous models: the attachment point theory and the engineered roughness index (ERI) model. The new surface energetic attachment (SEA) model is based on both the properties of the cell−material interface and the size and configuration of the topography relative to the organism. We have used Monte Carlo simulation to examine the SEA model's ability to predict relative attachment of the green alga *Ulva linza* to different locations within a unit cell. We have also compared the predicted relative attachment for *Ulva linza*, the diatom *Navicula incerta*, the marine bacterium *Cobetia marina*, and the barnacle cyprid *Balanus amphitrite* to a wide variety of microtopographies. We demonstrate good correlation between the experimental results and the model results for all tested experimental data and thus show the SEA model may be used as a powerful indicator of the efficacy for antifouling topographies.

INTRODUCTION

Microtopographic surfaces have gained much attention recently as potential nontoxic antifouling strategies to replace biocides in the marine environment.[1−6] The most recent literature has attempted to define a mechanism of antifouling. Configuration,[7−10] aspect ratio,[11] and feature size[12,13] are variables that have been identified. However, the relative importance of each and the mechanisms through which the different topographical characteristics control attachment have thus far proved to be elusive.

The attachment point theory was one of the earliest attempts to use topographic characteristics to predict organism attachment.[5,14,15] This theory is based on the empirical observation that organisms tend to attach in areas where they can maximize the number of contact points they can make with a surface, the logic being that these are the locations where the organism must expend the least amount of metabolic energy once attached. The theory is appealing for its simplicity and has been shown to apply at least in part to a variety of organisms.

Several attempts have been made to quantify the effect of attachment points.[2,15−17] However, these attempts illustrate the theory's shortcomings. Scardino et al.[15] showed that the number of attachment points was insufficient to predict a relative change in fouling for the diatom *Amphora sp.*, the green alga *Ulva rigida*, and the red alga *Centroceras clavulatum*; interestingly, it was effective for other organisms: the tubeworm *Hydroides elegans* and the bryozoan *Bugula neritina*. Quantitative predictions based on attachment point theory are complicated for those organisms that can "choose" between sites with differing numbers of attachment points (e.g., Figure 1). The theory does not provide a way to quantify these topographies in a meaningful way and can therefore only provide a useful observation for the development of other models.

In previous papers we have attempted to quantitatively predict fouling through the engineered roughness index (ERI) model,[7,18−20] which is based on the theories of wetting of a textured surface by Wenzel[21] and Cassie.[22] The ERI model relates the surface's Wenzel roughness r, the number of distinct features n, and the fractional area of feature tops φ_s from the Cassie equation through an experimentally fitted slope m to the relative attachment density of organisms to a patterned surface compared to smooth (N_t/N_s) (eq 1)

$$\ln\left(\frac{N_t}{N_s}\right) = -m\frac{rn}{1 - \varphi_s} = -m\mathrm{ERI}_{\mathrm{II}}$$

(1)

The ERI model relates the relative attachment density on a topography to the physical attributes of the surface through the
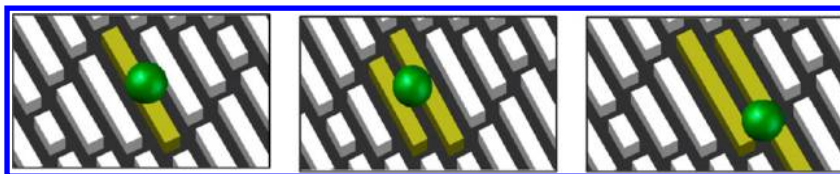
Figure 1. The unit cell seen here offers three different sites with different numbers of attachment points. Features that offer 1, 2, and 3 attachment points at each location are highlighted in yellow.

Wenzel and Cassie−Baxter wetting theories commonly applied to topographically modified surfaces. Equation 1 has been shown to be effective in predicting the relative attachment density of zoospores of the green alga *Ulva linza* to topographies with feature spacing and width less than the critical dimension of the spore (ca. 5 μm). The attachment density decreases logarithmically as the ERI value of the topography increases in the fashion predicted by eq 1.

The first application of the ERI model was limited in scope, only examining zoospores of *U. linza* on topographies cast in polydimethylsiloxane elastomer (PDMSe). Magin et al.[18,19] extended the ERI model to the bacterium *Cobetia marina* as well as a second chemistry in hydroxyethyl methacrylate-based hydrogels, by incorporating an organism's Reynold's number (*Re*) and the ratio between a standard surface energy and the test substrate's surface energy (γ_0/γ) (eq 2, Figure 2).

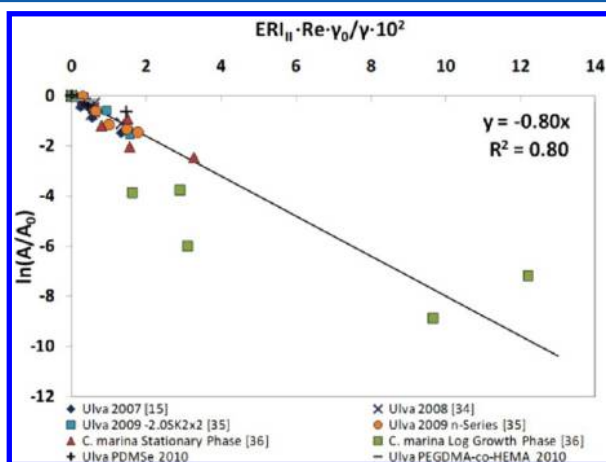$$\ln\left(\frac{N_t}{N_s}\right) = -m\frac{rn}{1 - \varphi_s}Re\frac{\gamma_0}{\gamma} \qquad (2)$$

Figure 2. Plot of relative settlement against eq 2. Image adapted with permission from ref 19.

The ERI predicts antifouling (i.e., inhibition of cell attachment) quite well ($R^2 = 0.80$) but fails to predict instances of fouling enhancement, i.e., increased attachment density of fouling organisms, as demonstrated in the recent paper by Xiao et al.[23] The Reynold's number term was included by Magin et al.[20] in an attempt to relate fouling to the size of the organism. However, the modified ERI still failed to predict increased attachment compared to a plain, unpatterned surface. These shortcomings simply highlight the empirical nature of the ERI and that the role of surface topography as a determinant of fouling is not adequately addressed.

In the present paper, we propose a new model that incorporates the concepts of the attachment point theory with the predictive capabilities of the ERI model into a unified model. Our model will show that single cell and multicellular organisms' response to topography is largely controlled by the contact area available for attachment as defined by Cassie−Baxter theory.

■ ANALYSIS

Different locations on the same topography can have a different number of attachment points and therefore must be treated differently using the attachment point theory (Figure 1). The topography must first be described in a way that will allow the investigation of individual locations in order to apply a quantitative model. This is accomplished by using a lattice model to describe different locations of the topography independently (Figure 3). Lattice models are a commonly employed technique used to compare systems with two or more interacting components and have found success in describing polymer mixing behavior, polymer graft conformations, magnetic properties, and other physical phenomena.[24]

The lattice model is effective because it allows for easy statistical analysis of a system based on discrete spatial relationships between the relevant system components. We applied this model to antifouling topographies by applying the lattice to the surface in a manner that allows the properties of a given site to be evaluated based upon the local conformation of the topography (Figure 3). A smooth surface and a topo-
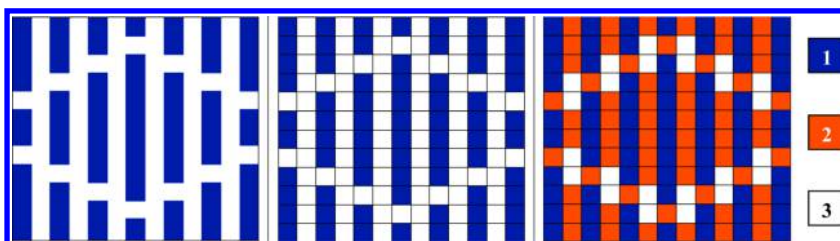

Figure 3. A lattice can be applied to the Sharklet AF unit cell in Figure 2 to accurately describe the differences between the sites. The left image is the unit cell. A lattice is applied to the unit cell in the middle image. The lattice can be divided based on the number of contact points an organism will have at that site, which is seen in the far right image. The blue sites have one contact point, the orange sites have two contact points, and the white sites have three contact points.

graphically modified surface were both examined in this way to elicit the inherent differences between these two types of surfaces.

The attachment point theory is ineffective because it provides no means to quantify the predicted amount of fouling. Therefore, the different sites must be described not only by their number of attachment points but also by the probability of attachment at each site due to those attachment points (Figure 3). Much of the biofouling literature indicates that certain surfaces, and locations on these surfaces, are more likely to accumulate fouling than others.[5,17,25−27] This effect cannot be explained as the result of statistical fluctuations. Rather, the literature indicates that fouling is most certainly not random and therefore must be controlled by the properties of the interface between the organism and the surface, namely the interfacial energy.

The field of statistical mechanics provides a useful set of tools for describing the probability of an event in terms of energy. Each site has a certain amount of interfacial area A that will result if an organism attaches at that site; this interfacial area is controlled entirely by the number of attachment points. The change in free energy ΔG_{123} to create a new interface in a three-component system can be related to A and the interfacial energy γ through eq 3:

$$\Delta G_{123} = A(\gamma_{13} - \gamma_{12} - \gamma_{23}) \tag{3}$$

The canonical ensemble was applied to calculate the probability (eq 4) of a site being filled by making the assumption that filled sites have only one cell and the temperature and volume for all cells are constant. This probability, i.e., N_t/N (the number of filled sites of a certain type (t) divided by the total number of filled sites), is dependent on the number of available sites g_t, the energy of each site E_t, and both temperature T and the partition function Z of the lattice.

$$\frac{N_t}{N} = \frac{g_t e^{-(E_t/kT)}}{Z} \tag{4}$$

$$Z = \sum_t g_t e^{-(E_t/kT)} \tag{5}$$

We can then compare two different types of lattice sites using eq 6.

$$\ln\left(\frac{N_t g_s}{N_s g_t}\right) = -\left(\frac{\Delta E_{ts}}{kT}\right) \tag{6}$$

The use of eq 6 permits the quantitative comparison of two surfaces for their AF potential. However, the comparison is complicated by the fact that the formation of interfaces is a function of both the surface properties and the organism. The organisms in this case cannot be described by the kT term. The energy of the organism extends beyond kT because its movement is directed and not defined by Brownian motion. So, we simply assign an "energy state" E_0 to replace kT (eq 7). This is expressed as

$$\ln\left(\frac{N_t g_s}{N_s g_t}\right) = -\left(\frac{\Delta E_{ts}}{E_0}\right) \tag{7}$$

A logical choice for E_0 in eq 7 is the attachment energy for whichever surface has been selected as a standard. For the studies examined in this paper, that surface is smooth polydimethylsiloxane elastomer (PDMSe). We substituted eq 3 into eq 7 to yield an equation that related surface parameters (contact area A and surface energy γ) to the relative settlement density.

$$\ln\left(\frac{N_t g_s}{N_s g_t}\right) = -\frac{\Delta(A(\gamma_{13} - \gamma_{12} - \gamma_{23}))_{ts}}{(A(\gamma_{13} - \gamma_{12} - \gamma_{23}))_s} \tag{8}$$

Equation 8 keeps the convention of using one of the test surfaces for the standard energy, surface "s" in this case. The end result is a normalized energy function that describes the relative attachment density of an organism between two surfaces. This normalized equation offers the benefit of not having to know the exact dimensions of an organism—rather, all that is necessary is the relative change between the surfaces. When the same surface chemistry is used, as is the case in the surfaces examined in this paper, eq 8 simplifies further to eq 9.

$$\ln\left(\frac{N_t g_s}{N_s g_t}\right) = \frac{\Delta A_{ts}}{A_s} \tag{9}$$

The subscripts t and s in eq 9 represent the value for the topographically modified surface and the smooth surface, respectively, and ΔA_{ts} is the difference between the interfacial areas of the organism on the topography and on a smooth surface. Equation 9 drops the negative sign in front of the energy expression to avoid misinterpreting the effect of area on attachment, since area cannot possibly be negative as opposed to the interfacial energy change, which is likely to be negative for the majority of surfaces.

An average area $\langle A_t \rangle$ can be used when comparing two surfaces with more than one type of site (Figure 3). The equations are the same, but the effect of a heterogeneous surface can be taken into account. Some slight rearrangement leads to the final form of the model (eqs 10 and 11).

$$\langle A_t \rangle = \frac{\sum_t (A_t g_t e^{-(E_t/E_0)})}{Z} \tag{10}$$

$$\ln\left(\frac{N_t}{N_s}\right) = \frac{\langle A_t \rangle - A_s}{A_s} + \ln\left(\frac{g_t}{g_s}\right) \tag{11}$$

Equation 11 represents a quantification of the attachment point theory, which we will refer to as the surface energetic attachment (SEA) model. This relation can easily be applied to existing data for validation as well as used as a tool in the preparation of new surfaces to either enhance or inhibit attachment.

The effectiveness of this model was investigated using four different organisms: zoospores of the green alga *Ulva linza* (*U. linza*), cells of the diatom *Navicula incerta* (*N. incerta*), the marine bacterium *Cobetia marina* (*C. marina*), and cypris larvae of the barnacle *Balanus amphitrite* (*B. amphitrite*). These four organisms differ in size, shape, and attachment mechanism, which enables them to be independently assessed using the proposed model. Validation of the model with *U. linza*, *N. incerta*, *C. marina*, and *B. amphitrite* provides a more complete picture of the relation between attachment area and relative attachment density for fouling organisms.

■ EXPERIMENTAL METHODS

Materials. The base material for the test surfaces in this study was SILASTIC T2 polydimethylsiloxane elastomer (PDMSe) from Dow Corning. SILASTIC T2 is a platinum-catalyzed silicone with good transparency and biocompatibility and is able to maintain feature fidelity for the duration of the attachment assays. The PDMSe is fabricated by mixing 10 parts resin to 1 part curing agent (by weight), followed by 5 min of mixing. The PDMSe mixture is then degassed under vacuum for 30 min, poured into topographical molds, and allowed to cure for 24 h at ambient conditions.

Pattern Selection. A wide variety of topographies were used to test the validity of the proposed model. The majority of the topographies are described elsewhere, and the attachment data for *U. linza, C. marina*, and *B. amphitrite* attachment are also taken from previously published literature.[7,8,11,12,20] Most of these patterns are based on the Sharklet AF microtopography, first described by Carman et al.[13] This topography consists of four distinct features which vary in length from 4 to 16 μm and have feature width and spacing of 2 μm. Several series of topographies have been fabricated to test the ERI model and have been included in the analysis for this study (Table 1 and Figures 4, 5, and 6).

Table 1. Literature References for Data Used To Validate the SEA Model

topography	source
ERI series	*Ulva*: Schumacher et al.[2]
	Marina: Magin et al.[18]
gradient series	Schumacher et al.[8]
N series	Long et al.[7]
wide series	Hoipkemeier-Wilson et al.[12]
aspect ratio	Schumacher et al.[11]
inverse SK	Long et al.[7]
channels and SK	Magin et al.[19]

Additional new patterns were fabricated to test the attachment of *N. incerta* (Figures 7 and 8). These patterns altered the size and spacing of the features in a systematic fashion in order to test the effect these parameters have on diatom attachment. The different feature dimensions effectively alter the A_t value for diatoms attaching to these topographies, making the evaluated topographies an excellent test of the SEA model for *N. incerta*.

Cell Attachment Data. *Navicula* cells were cultured in F/2 medium contained in 250 mL conical flasks. After 3 days the cells were in log phase growth. Cells were washed 3 times in fresh medium before harvesting and diluting to give a suspension with a chlorophyll *a* content of approximately 0.25 μg/mL. Cells were settled in individual dishes containing 10 mL of suspension at ~20 °C on the laboratory benches. Immediately, after addition of the diatom suspension, each dish was exposed to approximately 0.5 s of sonication to minimize
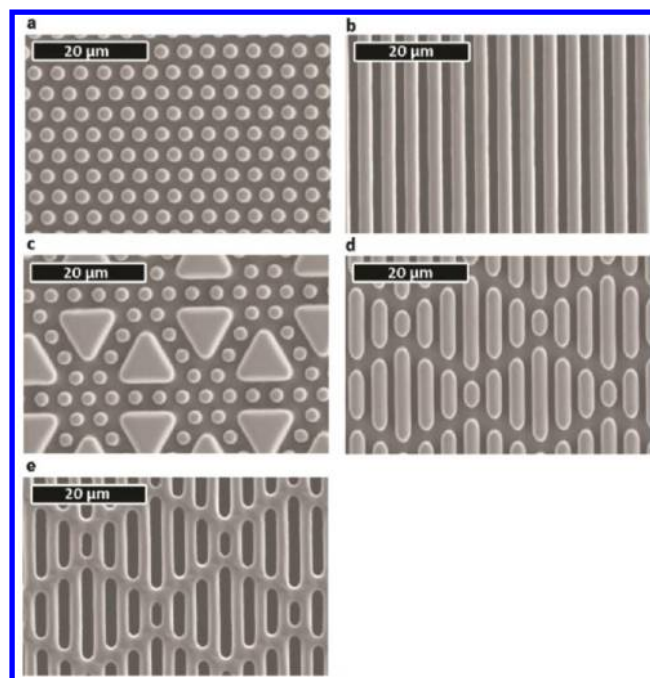

Figure 5. "ERI series" topographies, which systematically alter the r and φ_s values of a topography to alter the ERI value (eq 1). Topographies tested in Schumacher et al.[20]

entrapped air in the topographies. (In previous studies this has been shown not to damage cells or alter their behavior.) After 2 h the slides were gently washed in seawater to remove cells which had not properly attached. Samples were fixed in 2.5% glutaraldehyde and air-dried, and the density of cells attached to the surface was counted on each slide using an image analysis system attached to a fluorescence microscope. Counts were made for 30 fields of view (each 0.064 mm^2) on each slide.

The attachment data for zoospores of the green alga *U. linza,* the bacterium *C. marina,* and the barnacle cyprid *B. amphitrite* were taken from previously published results.[7,8,11,12,20] The data from refs 7, 8, and 20 have all been reported in previous papers from our group as having reduced attachment densities compared to smooth that can be predicted by the ERI model (eq 1). We have also included in our analysis the attachment data from Hoipkemeier-Wilson et al.[12] showing enhanced attachment of spores of *U. linza* relative to smooth on pillar and channel topographies of similar size to the spores as well as the attachment data for *U. linza* and *B. amphitrite* on patterns with different aspect ratios from Schumacher et al.[11] These data do not fit the ERI model and therefore provide good basis for analyzing the extent to which the SEA model can replace the ERI model for
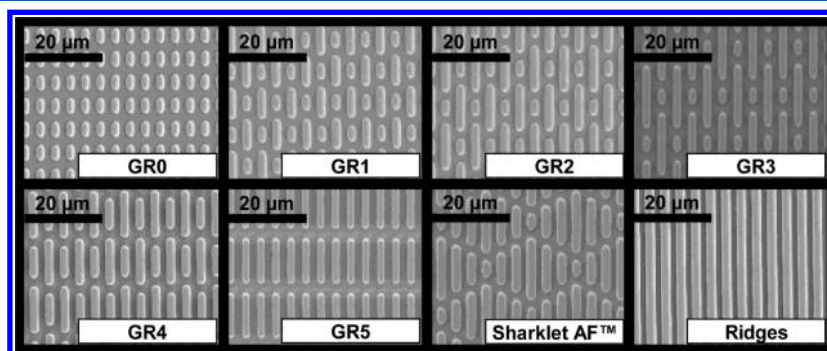

Figure 4. "Gradient series" topographies tested against *Ulva linza*. These topographies change the length ratio between two features, from 1:1 to 1:4. Topographies were tested in Schumacher et al.[8]
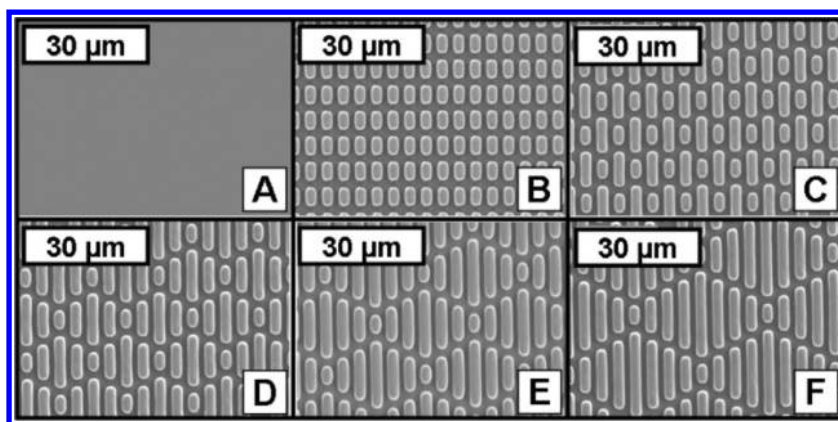
Figure 6. "N series" topographies which systematically alter the number of unique features (n) to change the surface's ERI value. Topographies tested against Ulva in Long et al.[7]
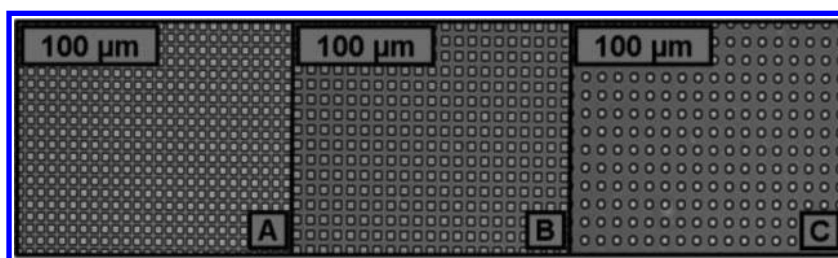

Figure 7. "Pillar series" topographies, which alter the spacing between features while leaving the number of features and size of features constant. These topographies were designed to test the relative area available for attachment of N. incerta.
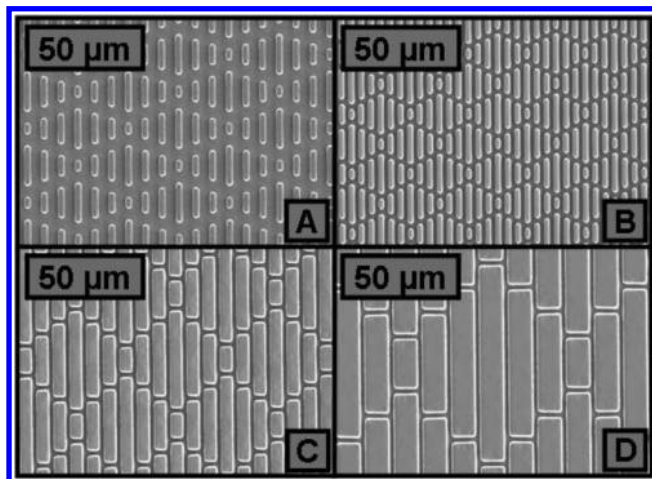

Figure 8. "S series" topographies, which alter the original Sharklet AF topography (topography B) by altering the spacing between features and the width of features. These topographies were designed to test the effect of feature size and spacing on attachment without altering the configuration of the topography.

predicting both enhanced and reduced cell attachment density on a variety of topographies.

Cell Attachment Area Calculations. Area calculations for U. linza attaching to topographies with spacing wider than the spore were made using the topography dimensions relative to an idealized version of the spore. Zoospores of U. linza are pyriform in shape while swimming and become spherical upon attachment. Zoospores are also pleiomorphic since the deformable membrane is not surrounded by a more rigid cell wall. However, to simplify calculations, for the purposes of this paper, zoospores were idealized as rigid spheres with 5 μm diameter.[18] The result of this simplification will be to underestimate the area of contact; however, the simplification did not introduce

appreciable error into the calculations. A spore in contact with a curved sidewall (i.e., a pillar) was assumed to have a contact area equal to half the value for its smooth counterpart. Spores were assumed to only attach in the spaces between topographic features due to the reported attachment pattern on these topographies.[5]

The relative attachment area for organisms attaching to topographies with width and spacing much (>2 μm) smaller or larger than the size of the organism (in this case, all organisms other than U. linza) was set to the φ_s value for the topography. Topographic dimensions were assumed to be constant throughout the patterned area and equal to the intended value stated in the reference. Measured dimensions deviate ± 0.2 μm from the intended value.[7,20] Topographies likely to be not fully wetted based on the predicted wetting states from the Wenzel and Cassie wetting equations at the time of the experiment were assigned a g_s/g_t value equal to $1/\varphi_s$ and set to one for all other topographies.

Simulation. A Monte Carlo simulation was performed using MATLAB software for points on a two-dimensional lattice. The simulation was meant to examine the SEA model's ability to predict attach maps of U. linza on narrow topographies. Metropolis Monte Carlo sampling was used to determine the equilibrium distribution of points on a topographic unit cell. The unit cell lattice was defined based on the asymmetric unit cell defined by Long et al.[17] (Figure 9), where each site was defined as 1 μm^2 with topography dimensions of 2 μm by 2 μm. Fixed boundary conditions were used to define the edges of the unit cell.

The site energy was defined by the attachment area, as seen in eq 3. The area of attachment predicted by using a "points of contact" simplification, where the number of contact points for a 5 μm diameter sphere at a site was used as the effective contact area. Probability was calculated by eq 9 with kT set to a reference value of one for a smooth surface as described previously. Equilibrium was determined by monitoring the ensemble energy at different simulation lengths.

Simulations were performed for 10 000 points for each topography. Points were randomly distributed to start the simulation. This number was selected because it provided good uniformity throughout the unit
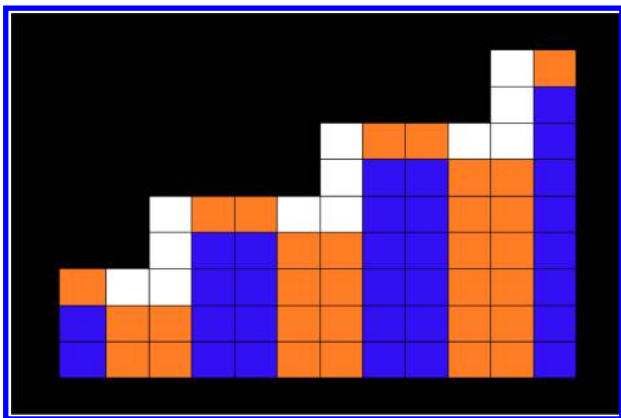
Figure 9. Asymmetric unit cell of the Sharklet topography. This asymmetric unit was introduced by Long et al.[17] as a method for modeling experimentally observed preferential attachment sites on engineered microtopographies. Blue sites have one contact point, orange sites have two, and white sites have three. Sites that are black exist in the simulation and are set to act as fixed boundary conditions.

cell at equilibrium while still allowing the simulation to run in a timely manner.

The output from each simulation was subsequently turned into a histogram using the method described by Long et al.[17] Briefly, this method involves assigning vector coordinates to each simulated cell relative to the origin of the unit cell (the lower left corner of Figure 9). These vector coordinates are then reflected and rotated to superimpose a histogram of cell density for each location over a representation of a topographic unit cell.

RESULTS AND DISCUSSION

The starting point selected for the evaluation of our SEA model was simulation of the attachment maps for zoospores of *U. linza*.[17] A simple Monte Carlo simulation gave a qualitative agreement between maps using the SEA model with those generated from the experimentally derived data (Figure 10).

The effectiveness of the SEA model is best demonstrated by its ability to represent experimentally determined preferential attachment sites (Figure 10). Furthermore, the model must predict attachment density as a function of the attachment area available to the organism. The change in attachment density between a smooth and patterned surface for *N. incerta, C. marina*, and *B. amphitrite* on narrow topographies (topographies with spacing smaller than the cell body) and zoospores of *U. linza* on both wide (spacing wider than the spore body) and narrow (spacing less than the spore body) topographies is predicted by the model with high correlation coefficient ($R^2 = 0.83$) and a slope of 1.05, near to the predicted value of 1 in eq 11 (Figure 11).

The results demonstrate that the SEA model predicts the attachment density for a number of different topographies and organisms. The model suggests the antifouling mechanism for effective topographies stems from the surface's ability to maintain the air pockets between the features, i.e., nonwetting state, which reduces the potential attachment sites (the $\ln(g_t/g_s)$ term in the model) for the cell/organism. This is consistent with our previous evaluations of the wetting/dewetting properties of these patterns[28] and corresponds with more recent observations made by other authors regarding antifouling topographies.[10,29] Conversely, the model suggests that the best way to increase cell attachment, such as for applications in aquaculture, is to present a topography that
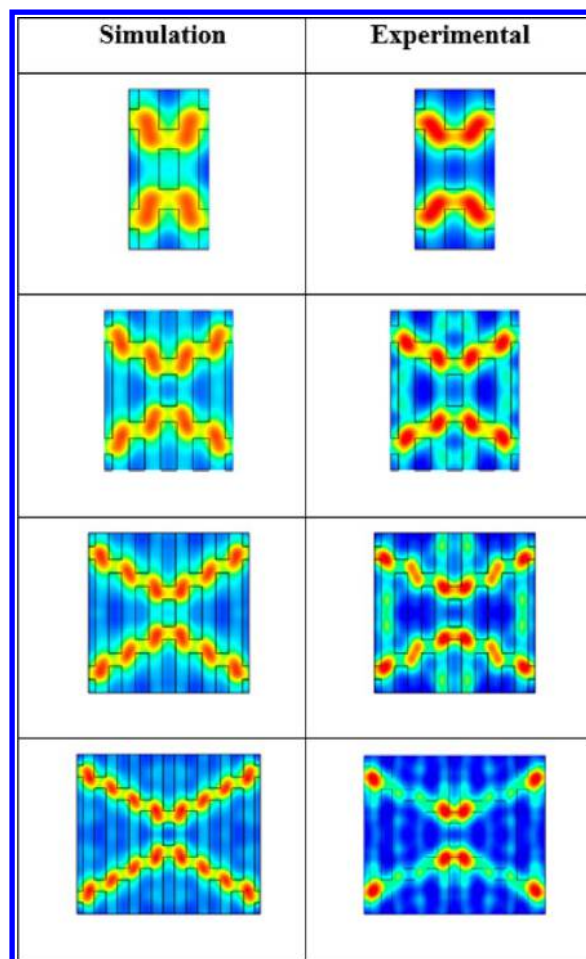

Figure 10. Comparison between simulated and experimentally measured attachment maps for *U. linza*. The simulated maps are seen in the left column and experimentally measured maps in the right column. In these maps, warm colors represent areas of relatively high attachment density, and cool colors represent areas of relatively low attachment density. These maps are for the "n series" topographies tested in Long et al.[7] and generated using the method of Long et al.[17]

maximizes attachment area. The model therefore predicts the observations that led to the attachment point theory.[15,16]

The attachment area changes based on the way organisms settled. Zoospores of *U. linza*, for example, attached to topographies with larger feature spacings by inserting themselves between the features, fully wetting the topography. This increases the attachment area "$a_{topography}$" such that it equals the surface area covered by the spore, which includes the sidewalls. Contrast this with the attachment area of the spore "a_{planar}" that attaches to a smooth surface. This allows us to simplify eq 11 so that the local r value of a site can be expressed in terms of the size of the organism (assuming the number of attachment sites is constant).

$$\ln\left(\frac{N_t}{N_s}\right) = \frac{a_{topography}}{a_{planar}} - \frac{a_{planar}}{a_{planar}} = r - 1 \tag{12}$$

Interestingly, eq 12 predicts an increase in attachment as r increases, which is the trend observed by Xiao et al.,[23] which incidentally also used topographies that were not accurately described by the ERI model. The case of cells of the diatom *N. incerta* attaching to topographies with narrow spacing is a special case of eq 12. In this scenario, the cells are only in
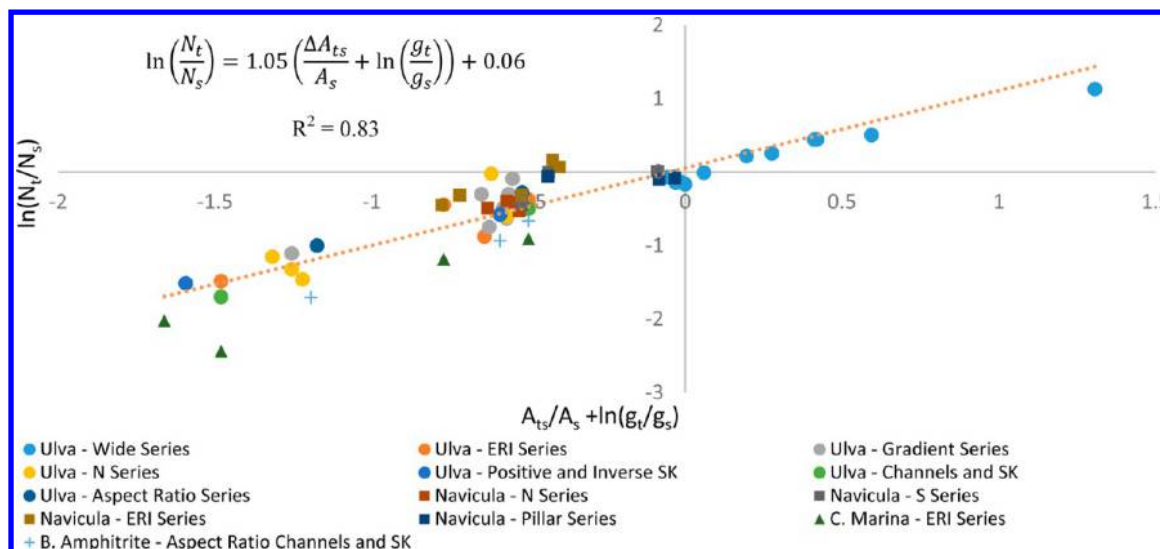
Figure 11. Comparison between the SEA model and experimentally measured attachment density data for *U. linza, N. incerta, C. marina,* and *B. amphitrite.* The data can be compared to eq 11. Sources for data seen in Table 1.

contact with the tops of the features. The *r* term is then equal to the fractional area of feature tops for the area covered by the cell (eq 13)

$$\ln\left(\frac{N_t g_s}{N g_t}\right) = \frac{a_{\text{topography}}}{a_{\text{planar}}} - \frac{a_{\text{planar}}}{a_{\text{planar}}} = \varphi_s - 1 \tag{13}$$

In both cases the term driving the relative attachment density in the SEA model is also found in the ERI model (eq 1): *r* for the case of zoospore attachment to wide topographies (and subsequent increase in attachment density) and φ_s for the case of diatom attachment to narrow topographies (and subsequent decrease in attachment density). The predictive power of the ERI model for certain topographies is potentially derived from these similarities.

Interestingly, these two regimes correspond to the analogous regime for a liquid spreading on a topography. The spore, which settles between features, effectively "wets" all of the available surface area. The attachment density of these spores is best described by the Wenzel term and is analogous to a liquid that is in "the Wenzel non-wetting state". Conversely, the diatom cell attachment only "wets" the tops of features. Thus, the surface area of contact, for the diatom, is best described by the φ_s term in an analogous manner to a liquid in "the Cassie wetting state".

CONCLUSIONS

The surface energetics attachment (SEA) model, described in this article, represents the first time one is able to predict both enhancement of cell attachment and inhibition of cell attachment to a microtopography. The SEA model is based upon statistical mechanics, in which the probability of attachment was related to the relative attachment energy at a specific site. The attachment energy for different topographies was estimated in a simple way by relating attachment energy to attachment area. The relative attachment area was also shown to be a good predictor of both total attachment density for four disparate organisms, zoospores of *Ulva linza*, the benthic diatom *Navicula incerta*, the marine bacterium *Cobetia marina*, and cypris larvae of the barnacle *Balanus amphitrite*. Interestingly, all four species follow the same relationship

with attachment area, indicating that this model may be applied to a wide variety of applications, including aquaculture and antifouling coating technologies. We believe that this approach offers the opportunity to further develop antifouling strategies that are nontoxic, environmentally neutral, and more stable in a biological environment.

AUTHOR INFORMATION

Corresponding Author

*Ph (352) 392-6281, Fax (352) 392-3771, e-mail abrennan@ mse.ufl.edu (A.B.B.).

Notes

The authors declare no competing financial interest.

REFERENCES

(1) Carl, C.; Poole, A.; Sexton, B. A.; Glenn, F.; Vucko, M. J.; Williams, M.; Whalan, S.; De Nys, R. Enhancing the settlement and attachment strength of pediveligers of Mytilus galloprovincialis bychanging surface wettability and microtopography. *Biofouling* **2012**, *28*, 175−186.

(2) Aldred, N.; Scardino, A.; Cavaco, A.; De Nys, R.; Clare, A. S. Attachment strength is a key factor in the selection of surfaces by barnacle cyprids (Balanus amphitrite) during settlement. *Biofouling* **2010**, *26*, 287−299.

(3) Bloecher, N.; de Nys, R.; Poole, A. J.; Guenther, J. The fouling hydroid Ectopleura larynx: a lack of effect of next generation antifouling technologies. *Biofouling* **2013**, *29*, 237−246.

(4) Scardino, A. J.; de Nys, R. Mini review: Biomimetic models and bioinspired surfaces for fouling control. *Biofouling* **2011**, *27*, 73−86.

(5) Callow, M. E.; Jennings, A. R.; Brennan, A. B.; Seegert, C. E.; Gibson, A.; Wilson, L.; Feinberg, A.; Baney, R.; Callow, J. A. Microtopographic cues for settlement of zoospores of the green fouling alga Enteromorpha. *Biofouling* **2002**, *18*, 229−236.

(6) Cooper, S. P.; Finlay, J. A.; Cone, G.; Callow, M. E.; Callow, J. A.; Brennan, A. B. Engineered antifouling microtopographies: kinetic

analysis of the attachment of zoospores of the green alga Ulva to silicone elastomers. *Biofouling* **2011**, *27*, 881−892.

(7) Long, C. J.; Schumacher, J. F.; Robinson, P. A. C.; Finlay, J. A.; Callow, M. E.; Callow, J. A.; Brennan, A. B. A model that predicts the attachment behavior of Ulva linza zoospores on surface topography. *Biofouling* **2010**, *26*, 411−419.

(8) Schumacher, J. F.; Long, C. J.; Callow, M. E.; Finlay, J. A.; Callow, J. A.; Brennan, A. B. Engineered nanoforce gradients for inhibition of settlement (attachment) of swimming algal spores. *Langmuir* **2008**, *24*, 4931−4937.

(9) Efimenko, K.; Finlay, J.; Callow, M. E.; Callow, J. A.; Genzer, J. Development and testing of hierarchically wrinkled coatings for marine antifouling. *ACS Appl. Mater. Interfaces* **2009**, *1*, 1031−1040.

(10) Wu, A. H.; Nakanishi, K.; Cho, K.; Lamb, R. Diatom attachment inhibition: limiting surface accessibility through air entrapment. *Biointerphases* **2013**, *8*, 1−10.

(11) Schumacher, J. F.; Aldred, N.; Callow, M. E.; Finlay, J. A.; Callow, J. A.; Clare, A. S.; Brennan, A. B. Species-specific engineered antifouling topographies: correlations between the settlement of algal zoospores and barnacle cyprids. *Biofouling* **2007**, *23*, 307−317.

(12) Hoipkemeier-Wilson, L.; Schumacher, J. F.; Carman, M. L.; Gibson, A. L.; Feinberg, A. W.; Callow, M. E.; Finlay, J. A.; Callow, J. A.; Brennan, A. B. Antifouling potential of lubricious, micro-engineered, PDMS elastomers against zoospores of the green fouling alga Ulva (Enteromorpha). *Biofouling* **2005**, *20*, 53−63.

(13) Carman, M. L.; Estes, T. G.; Feinberg, A. W.; Schumacher, J. F.; Wilkerson, W.; Wilson, L. H.; Callow, M. E.; Callow, J. A.; Brennan, A. B. Engineered antifouling microtopographies−correlating wettability with cell attachment. *Biofouling* **2006**, *22*, 11−21.

(14) Verran, J.; Boyd, R. D. The relationship between substratum surface roughness and microbiological and organic soiling: a review. *Biofouling* **2001**, *17*, 59−71.

(15) Scardino, A. J.; Guenther, J.; De Nys, R. Attachment point theory revisited: the fouling response to a microtextured matrix. *Biofouling* **2008**, *24*, 45−53.

(16) Scardino, A.; Harvey, E.; De Nys, R. Testing attachment point theory: diatom attachment on microtextured polyimide biomimics. *Biofouling* **2006**, *22*, 55−60.

(17) Long, C. J.; Finlay, J. A.; Callow, M. E.; Callow, J. A.; Brennan, A. B. Engineered antifouling microtopographies: mapping preferential and inhibitory microenvironments for zoospore attachment. *Biofouling* **2010**, *26*, 941−952.

(18) Magin, C. M.; Long, C. J.; Cooper, S. P.; Ista, L. K.; López, G. P.; Brennan, A. B. Engineered antifouling microtopographies: the role of Reynolds number in a model that predicts attachment of zoospores of Ulva and cells of Cobetia marina. *Biofouling* **2010**, *26*, 719−727.

(19) Magin, C. M.; Finlay, J. A.; Clay, G.; Callow, M. E.; Callow, J. A.; Brennan, A. B. Antifouling performance of cross-linked hydrogels: refinement of an attachment model. *Biomacromolecules* **2011**, *12*, 915−922.

(20) Schumacher, J. F.; Carman, M. L.; Estes, T. G.; Feinberg, A. W.; Wilson, L. H.; Callow, M. E.; Callow, J. A.; Finlay, J. A.; Brennan, A. B. Engineered antifouling microtopographies−effect of feature size, geometry, and roughness on settlement of zoospores of the green alga Ulva. *Biofouling* **2007**, *23*, 55−62.

(21) Wenzel, R. N. Resistance of solid surfaces to wetting by water. *Ind. Eng. Chem.* **1936**, *28*, 988−994.

(22) Cassie, A. B. D.; Baxter, S. Wettability of porous surfaces. *Trans. Faraday Soc.* **1944**, *40*, 546−551.

(23) Xiao, L.; Thompson, S.; Rohrig, M.; Callow, M. E.; Callow, J. A.; Grunze, M.; Rosenhahn, A. Hot embossed microtopographic gradients reveal morphological cues that guide the settlement of zoospores. *Langmuir* **2013**, *29*, 1093−1099.

(24) Baxter, R. J. *Exactly Solved Models in Statistical Mechanics*; Dover Publications: Mineola, NY, 2007.

(25) Ista, L. K.; Callow, M. E.; Finlay, J. A.; Coleman, S. E.; Nolasco, A. C.; Simons, R. H.; Callow, J. A.; Lopez, G. P. Effect of substratum surface chemistry and surface energy on attachment of marine bacteria and algal spores. *Appl. Environ. Microbiol.* **2004**, *70*, 4151−4157.

(26) Carl, C.; Poole, A. J.; Williams, M. R.; de Nys, R. Where to settle—settlement preferences of Mytilus galloprovincialis and choice of habitat at a micro spatial scale. *PLoS One* **2012**, *7*, e52358.

(27) Magin, C. M.; Cooper, S. P.; Brennan, A. B. Non-toxic antifouling strategies. *Mater. Today* **2010**, *13*, 36−44.

(28) Long, C. J.; Schumacher, J. F.; Brennan, A. B. Potential for tunable static and dynamic contact angle anisotropy on gradient microscale patterned topographies. *Langmuir* **2009**, *25*, 12982−12989.

(29) Friedlander, R. S.; Vlamakis, H.; Kim, P.; Khan, M.; Kolter, R.; Aizenberg, J. Bacterial flagella explore microscale hummocks and hollows to increase adhesion. *Proc. Natl. Acad. Sci. U. S. A.* **2013**, *110*, 5624−5629.